LBL-26005

Lawrence Berkeley Laboratory

UNIVERSITY OF CALIFORNIA

Accelerator & Fusion Research Division

Presented at the 1988 Summer Study on High Energy Physics in the 1990's, Snowmass, CO, June 27–July 15, 1988

Design of 9 T 5 cm Bore Dipole

C.E. Taylor and S. Caspi

July 1988

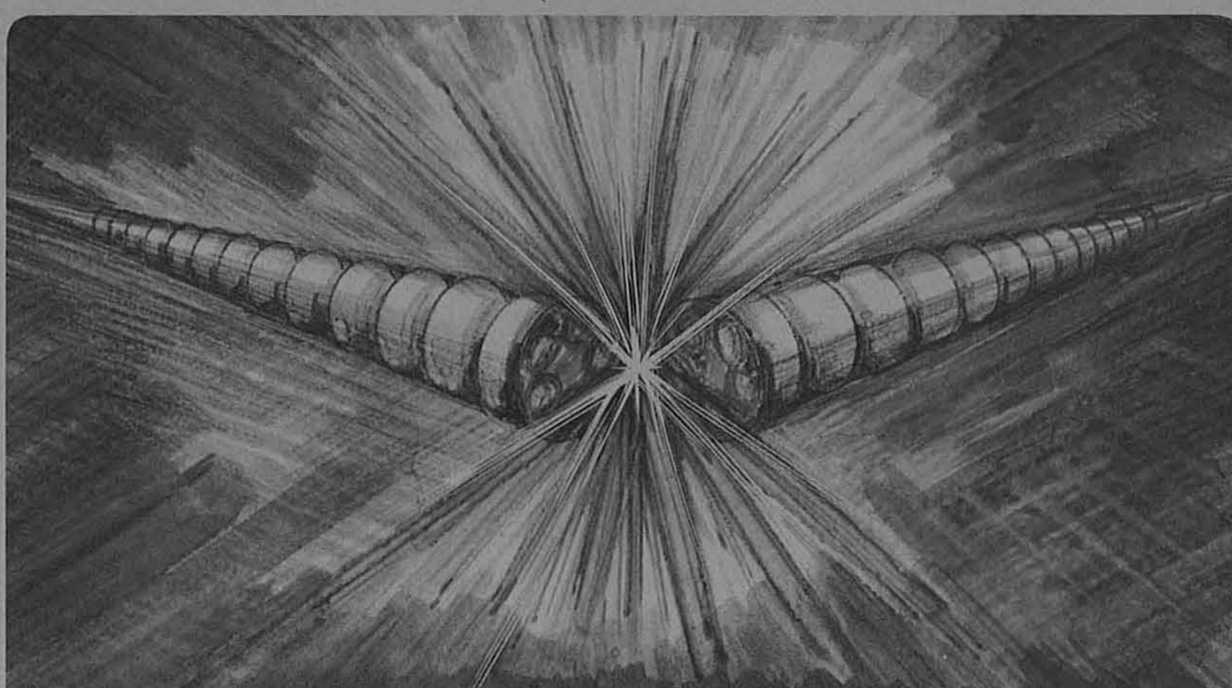

Prepared for the U.S. Department of Energy under Contract Number DE-AC03-76SF00098.

LBL-26005
SSC-MAG-207

DESIGN OF A 9 T 5 CM BORE DIPOLE*

Clyde E. Taylor and Shlomo Caspi

Accelerator and Fusion Research Division
Lawrence Berkeley Laboratory
1 Cyclotron Road
Berkeley, California 94720

1988 Summer Study on High Energy Physics in the 1990's
Snowmass, Colorado, June 27 - July 15, 1988

*This work was supported by the Director, Office of Energy Research, Office of High Energy and Nuclear Physics, High Energy Physics Division, U.S. Dept. of Energy, under Contract No. DE-AC03-76SF00098.

DESIGN OF A 9T 5 CM BORE DIPOLE*

Clyde E. Taylor and Shlomo Caspi

Lawrence Berkeley Laboratory
University of California
Berkeley, California 94720

INTRODUCTION

A conceptual design is presented for an accelerator dipole magnet intended for a collider application with central field of 9T and a coil bore diameter of 5 cm.. Figure 1 shows a schematic cross-section of the collared coil in a circular cold iron yoke. Emphasis is on identifying a superconducting cable and a coil design that requires little development and which will result in a reasonable operating "margin". Conventional NbTi superconducting cable is used, operating at 2 K to increase the critical current density. The cable and strand proposed are similar to designs now being manufactured for the SSC and the Tevatron. Figure 2 shows a comparison with the 6.6T, 4.35 K SSC dipole.

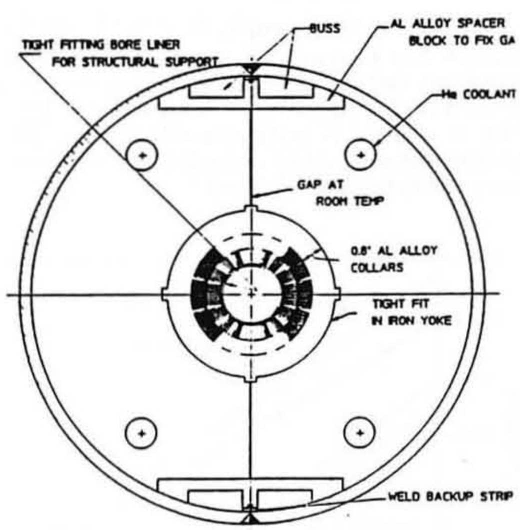

Fig. 1 Schematic of 9T 5 cm bore cold-iron dipole magnet design.

*This work was supported by the Director, Office of Energy Research, Office of High Energy and Nuclear Physics, High Energy Physics Division, U.S. Dept. of Energy, under Contract No. DE-AC03-76SF00098.

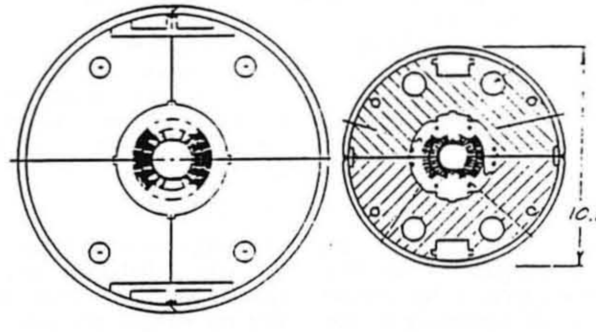

Fig. 2 Comparison of this design with the SSC design - both are shown to the same scale.

CABLE DESIGN

Recent R&D aimed at the Superconducting Super Collider (SSC) has resulted in reliable production of long cable lengths with high J_c. A superconducting strand design is selected that is similar to strands now being manufactured in quantity. Table I gives the strand and cable parameters used in this design for the SSC program.

TABLE I

INNER

Strand Diameter	0.0318 in.
Cu/SC ratio	1.3
Filament diameter	6 μm
Twist	1-2 per in.
Number strands	30
Keystone angle	1.23 deg.
Thickness	0.0522 in., 0.0625 in.
Width	0.477 in.

OUTER

Strand Diameter	0.0268 in.
Cu/SC ratio	1.8
Filament diameter	6 μm
Twist	1-2 per in.
Number strands	36
Keystone angle	1.01 deg.
Thickness	0.0438 in., 0.0522 in.
Width	0.477 in.

Note the inner strand is identical to the SSC R&D strand. The outer strand is identical to that now being used for the Tevatron. However, compared to SSC inner and outer cables, these are wider and have a 1.3 times greater cross-sectional area. The inner has 30 strands (rather than 23); 30 strand cable is now being made for the SSC outer layer. The outer strand diameter is 0.0268 in. (the Tevatron strand size) and 36 strands are used; 36 strand cable is now being made at LBL for the Tevatron low-b quadrupoles. Both cables can be made in quantity with minimal development.

GENERAL DESCRIPTION OF THE MAGNET (COLD MASS)

Structural support of the 2-layer, graded, "cos q" coils, is provided by aluminum alloy collars that provide part of the required compression of the coils during assembly; a split cold-iron yoke fits closely around the collars supporting the magnetic forces and providing additional coil compression as shown in Fig. 1. The yoke is split at the vertical plane and a small gap is deliberately maintained at assembly by an aluminum alloy spacer bar. During cool-down, the gap closes as the collared coil shrinks more than the iron yoke. The gap thickness at assembly is precisely determined by the spacer bar. The yoke is enclosed in a stainless steel tube which maintains the required force on both the collared coil and spacer bar during assembly, cooldown, and operation. Figure 1 shows a yoke with a circular outer boundary; this shape as shown has excess iron cross section in the pole region; optimized cross sections with less iron could be elliptical in shape with the same midplane width.

COIL CROSS-SECTION

The coil is a 2-layer cos q design very similar to the one proposed for the SSC. The cable is slightly keystoned and copper wedges are used to provide the arch structure that is self-supporting on the inside; the wedges also provide proper conductor placement for uniform central field. The outer cable results in a higher current density because it experiences a lower field. This design is similar to the SSC design and gives a very uniform field (i.e., small "systematic" or built-in field distortion); Fig. 3 shows the 4-wedge cross section with 18 inner turns per coil and 27 outer turns per coil. The inner-layer wedges are between turns 3 and 4; turns 7 and 8, and turns 13 and 14. The outer layer edge is between turns 19 and 20.

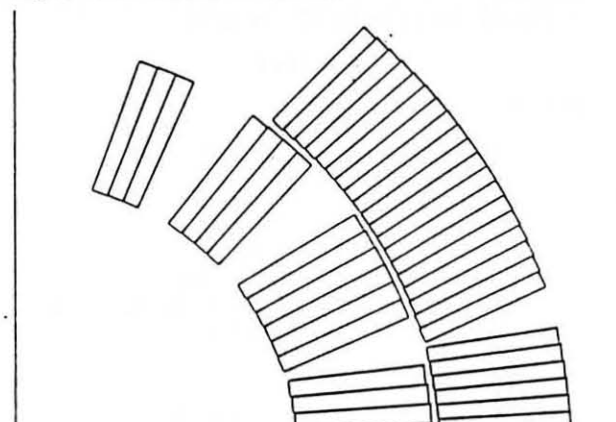

Fig. 3. Quadrant showing conductor layout for the 5 cm bore diameter cross-section, showing the inner layer with 18 turns and 3 wedges and the outer layer with 27 turns and one wedge.

COLLARS AND YOKE

The aluminum alloy collars are assembled around the coils using tapered keys (as in the SSC) producing an azimuthal compression of about 10 kpsi. The split yoke is assembled tightly around the collars with a small gap (~0.5 mm) in the vertical plane; during this assembly some additional compression may be applied to the coils. Upon cooldown, as the coil contracts more than the yoke, the gap closes so as to increase the compressive stress to a predetermined value because the spacer bar, which determines the gap size, also contracts proportionally. We estimate that about 12 kpsi total prestress is needed. The thermal contraction of the stainless steel shell is sufficient to provide the required forces. The yoke gap can as well be placed at the horizontal mid-plane; such a horizontal gap reduces the relative azimuthal sliding between collars and yoke as the gap closes; however, in this case, the aluminum spacer bars, which would span the gap on the sides of the yoke, would require the horizontal yoke dimension to be somewhat greater to provide sufficient iron for the return flux path. The yoke as shown is wide enough to achieve a minimum leakage field with a central field of 9T.

SUPERCONDUCTOR

For this design, an operating temperature of 2 K is chosen because of the very significant increase in J_c as temperature is reduced. Pressurized helium would be pumped through passages in the yoke and recooled at intervals around the ring. A design has not been made for the refrigeration system; however, large-scale 2 K refrigeration plants have been built and the design problems appear straightforward. The magnet test facility at Fermilab has recently been modified to permit circulation of 1.8 K pressurized helium.

Figure 4 from reference 1 shows J_c vs. B for recently produced Nb46.5wt% Ti (the "standard alloy") at 4.2 K and 1.8 K; also shown for comparison is data for a Nb45wt% Ti15wt% Ta ternary alloy.

For the NbTi sample, J_c at 4.2 K and 5T is 2800 A/mm^2 (the present SSC specification is 2750 A/mm^2 minimum); note that at 1.8 K and 8T, J_c is the same as at 4.2 K and 5T. The data of Fig. 4 is redrawn in Fig. 5(a) and 5(b), in which 2 K performance is shown. The 2 K J_c prediction is obtained by a simple linear (and conservative) interpolation between 4.2 K and 1.8 K.

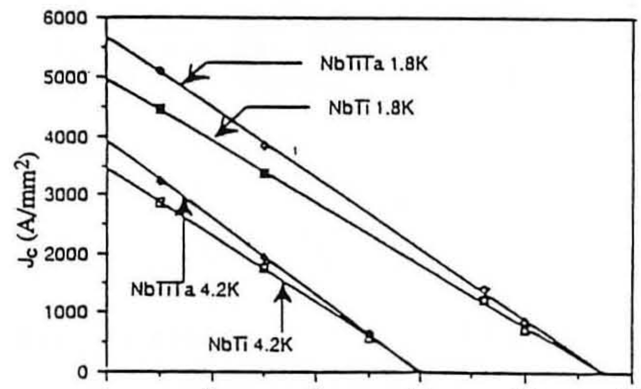

Fig. 4 J_c vs. field at 4.2 K and 1.8 K for test billets of NbTi and NbTiTa (Ref. 1).

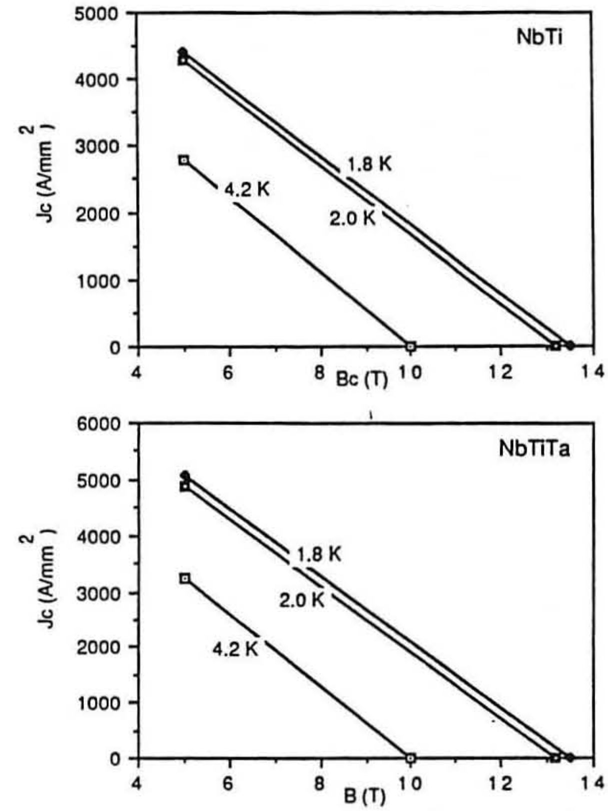

Figs. 5(a) and 5(b) J_c vs. B derived from Fig. 4

Figure 6 shows magnet current I vs. central field B_o, and maximum field B_m at the inner coil. Also shown on the same graph are critical current vs. field for the inner cable for both the NbTi and the NbTiTa alloys. The intersection of the magnet load line, I vs. B_m, with the critical current line determines the critical current (or "short sample" current). The outer cable is designed to quench at a slightly higher current than the inner cable. For this design, Fig. 6 indicates that at 2 K for NbTi, the critical current is 10.4 kA when B_m is 10.2T and B_o = 9.65T. For B_o = 9.0T, I = 9.53 kA while the cable critical current is 12.8 kA. This should be an adequate operating margin at B_o = 9.0T to allow for the myriad of unavoidable departures from "ideal" conditions.

The ternary alloy (Nb45wt%Ni15wt%Ta) has been studied for high field applications, but, to date, has been made in small quantities. Addition of Ta results in a higher cost than for the NbTi alloy, but, as seen in Fig. 4, higher J_c is observed. This material is now being studied to determine the optimum properties that can be obtained from various compositions. It appears to be ductile and can be easily drawn and cabled as can NbTi.

Figure 6 shows that the critical field of this design is 9.95T with the NbTiTa alloy at 2 K.

MAGNETIZATION AND FIELD QUALITY

The built-in systematic field distortion is very small; the calculated $\frac{\Delta B}{B}$ for this design is 2 x 10^{-5}. Since the magnet is similar to the SSC design, the expected random multipoles at 1.25 cm (half the coil inner radius) should be about the same as for the SSC at 1.0 cm.[2]

At fields above about 5 T, saturation results in field distortion that is characterized by the normal sextupole component of the field; Fig. 7 shows the sextupole harmonic, b_2, vs. the central dipole field b_o as calculated by the computer code POISSON; $b_2 = B_2/B_o \times 10^{-4}$ where B_2 is the intensity of the sextupole field component. All higher order multipoles have saturation effects less than 10^{-5}. A field line plot is calculated by POISSON shown in Fig. 8.

For filaments of about 6 μm diameter, we expect the field distortion magnetization at very low (injection) field to be similar to that of SSC models with the same filament size. However, the increased J_c at 2 K should result in increased magnetization at constant field. Figure 9 shows sextupole harmonics measured at LBL in a 1-m SSC model[3] at 4.3 K and at 1.8 K; the additional magnetization effect at lower temperature can be seen.

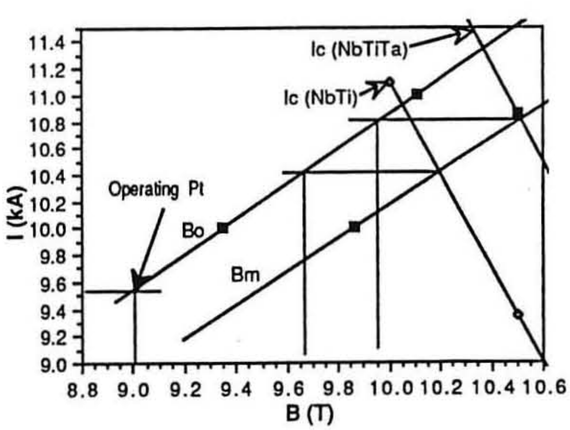

Fig. 6 Load line and critical curve for 9T, 2 K dipole.

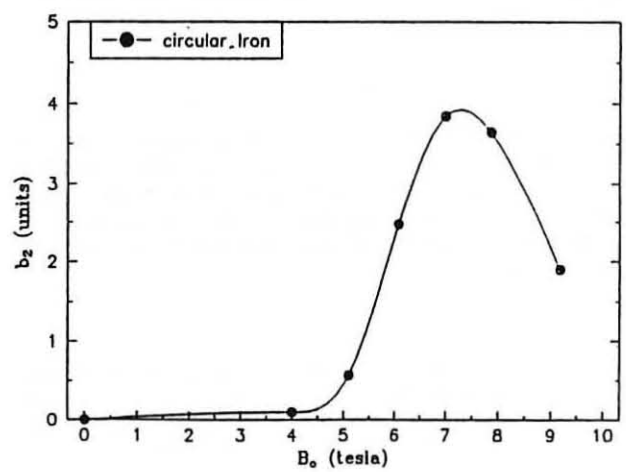

Fig. 7. The Effect of Iron Saturation Effect on b_2.

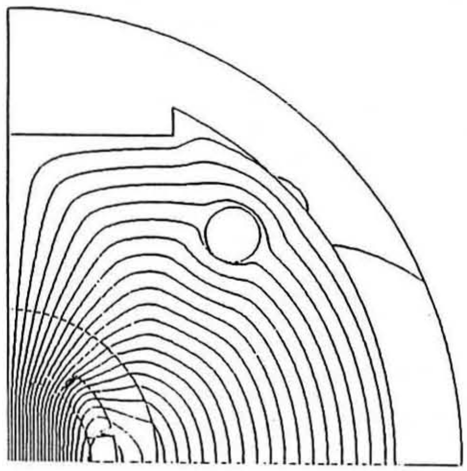

Fig. 8 Field lines calculated with POISSON.

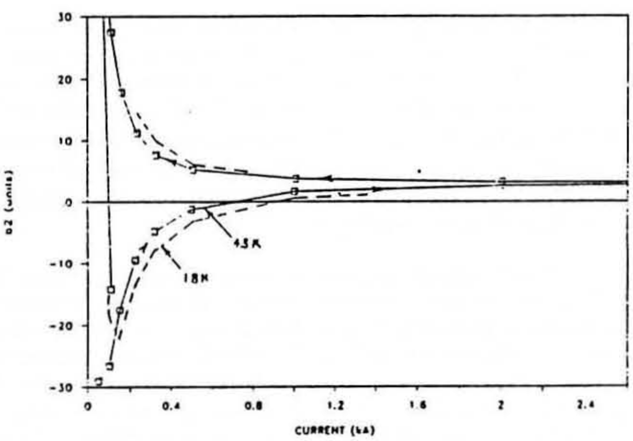

Fig. 9 Sextupole vs. current measured in 1-m SSC Model D15A-5.

CONCLUSIONS

We note that SSC dipole models, although designed for 6.6 T operating field at 4.35 K, have achieved central fields greater than 9T at 1.8 K[4]; for this design, with wider cable, additional iron, and proper mechanical support, a 9T operating field should be possible with reasonable margin as shown by the above results.

REFERENCES

1. E. Gregory, et al., "Preliminary Properties of Ductile Superconducting Alloys at 10T and Above," presented at the International Conference on Cryogenic Engineering, ICEC-12, Southampton, U.K.; July 12, 1988.

2. SSC Central Design Group, "Conceptual Design of the Superconducting Super Collider," SSC-SR-2020, March, 1986.

3. W. Gilbert and P. Barale, "Prompt Report on LBL-SSC Model Magnet D-15A-5," SSC-MAG-196, LBID-1400, April 25, 1988.

4. W. Gilbert and P. Barale, "Prompt Report on LBL-SSC Model Magnet D15A-3, SSC-MAG-170, LBID-1333, November 1, 1987 (for example).